Structural Basis of Multiple Drug-Binding Capacity of the AcrB Multidrug Efflux Pump

Edward W. Yu, *et al.*

Science **300**, 976 (2003);
DOI: 10.1126/science.1083137

Science (print ISSN 0036-8075; online ISSN 1095-9203) is published weekly, except the last week in December, by the American Association for the Advancement of Science, 1200 New York Avenue NW, Washington, DC 20005.

Structural Basis of Multiple Drug-Binding Capacity of the AcrB Multidrug Efflux Pump

Edward W. Yu,[1] Gerry McDermott,[2]
Helen I. Zgurskaya,[1]* Hiroshi Nikaido,[1] Daniel E. Koshland Jr.[1]†

Multidrug efflux pumps cause serious problems in cancer chemotherapy and treatment of bacterial infections. Yet high-resolution structures of ligand-transporter complexes have previously been unavailable. We obtained x-ray crystallographic structures of the trimeric AcrB pump from *Escherichia coli* with four structurally diverse ligands. The structures show that three molecules of ligands bind simultaneously to the extremely large central cavity of 5000 cubic angstroms, primarily by hydrophobic, aromatic stacking and van der Waals interactions. Each ligand uses a slightly different subset of AcrB residues for binding. The bound ligand molecules often interact with each other, stabilizing the binding.

Multidrug efflux pumps are now known to be present in most living cells. In human cells, pumps such as P-glycoprotein prevent the entry of toxic molecules at the mucosal surface of the intestinal tract or at the blood-brain barrier. When overexpressed, P-glycoprotein makes cancer cells resistant to a wide range of anticancer agents (*1*). In bacteria, resistance to drugs is often associated with multidrug transporters functioning to decrease cellular drug accumulation (*2*, *3*). Understanding the broad chemical specificity of these transporters has challenged our scientific community for decades. The central issue concerns the nature of substrate recognition. Important suggestions came from the study of ligand binding to soluble regulatory proteins of bacterial multidrug efflux pumps. The regulatory domain of the *Bacillus subtilis* BmrR regulator was crystallized in the presence of an inducer tetraphenylphosphonium (*4*). The binding was shown to involve mostly hydrophobic interactions with some electrostatic effects in a relatively large and loose binding site. The subsequent study of the *Staphylococcus aureus* QacR regulatory protein (*5*) showed conclusively that different ligands bind to different parts of a large and flexible binding site, each time again relying mostly on hydrophobic interactions. However, the structural basis of drug binding to transporters themselves has never been elucidated.

Escherichia coli AcrB is a transporter that is energized by proton-motive force and that shows the widest substrate specificity among all known multidrug pumps, ranging from most of the currently used antibiotics, disinfectants, dyes, and detergents to simple solvents (*2*, *3*). Since its discovery (*6*), its properties have been studied by reconstitution (*7*), and it has served as a prototype bacterial multidrug transporter for studies of drug-transport mechanisms. Its ligand-free, trimeric structure was determined recently by x-ray crystallography in the laboratory of Yamaguchi (*8*), and this work has opened the approach to inquiry on the structural details of drug capture and transport. We have now solved the AcrB structure at a resolution of 3.5 to 3.8 Å in a complex with four different ligand molecules (Table 1). Our study shows that each ligand binds to different locations in the central cavity of the transmembrane domain of the trimer, not only confirming and extending the prediction of Brennan and coworkers on the nature of multidrug binding sites (*5*) but also showing small conformational changes in the protein upon substrate binding.

The structure of ligand-free AcrB (*8*) shows that it is a homotrimer of ~110 kD per subunit. Each subunit contains 12 transmembrane helices and two large periplasmic domains (each exceeding 300 residues) between helices α1 and α2, and helices α7 and α8 (*6*). X-ray analysis of the overexpressed AcrB protein demonstrated that the three periplasmic domains form, in the center, a funnel-like structure and a connected narrow (or closed) pore (Fig. 1). The pore is opened to the periplasm through three vestibules located at subunit interfaces. These vestibules were proposed to allow direct access of drugs from the periplasm as well as the outer leaflet of the cytoplasmic membrane (*8*). The three transmembrane domains of AcrB protomers form a large, 30Å-wide central cavity that spans the cytoplasmic membrane and extends to the cytoplasm (*8*).

We purified the wild-type AcrB (*9*) (without any "tags") and crystallized it in the presence of four structurally dissimilar agents, rhodamine 6G (R6G), ethidium (Et), dequalinium (Dq), and ciprofloxacin (Cip). The agents were added at 50 μM. In vitro reconstitution studies (*7*) showed that for most drugs, concentrations of ≥100 μM are needed to achieve 50% inhibition of the AcrB-catalyzed phospholipid-extrusion reaction. Thus, the drug concentrations used were modest in relation to the expected affinity of AcrB to these ligands.

The crystal structures illustrate that these ligands bind to various positions of the central cavity (Fig. 1 and Fig. 2), each using a different subset of residues (Fig. 2), thus greatly increasing the range of potential drug-protein interactions. (The electron density maps of the ligands are shown in Fig. 3.) The interior surface of the upper part of the cavity

Table 1. Data collection and crystallographic analysis.

Parameter	Unliganded	AcrB-R6G	AcrB-Et	AcrB-Dq	AcrB-Cip
Space group	*R*32	*R*32	*R*32	*R*32	*R*32
Cell constants (Å)	$a = b =$ 143.5, $c =$ 519.6, $\alpha = \beta = 90$, $\gamma =$ 120	$a = b =$ 144.8, $c =$ 518.6, $\alpha = \beta = 90$, $\gamma =$ 120	$a = b =$ 144.7, $c =$ 517.5, $\alpha = \beta = 90$, $\gamma =$ 120	$a = b =$ 144.8, $c =$ 517.9, $\alpha = \beta = 90$, $\gamma =$ 120	$a = b =$ 145.1, $c =$ 517.2, $\alpha = \beta = 90$, $\gamma =$ 120
Resolution (Å)	3.70 (3.83–3.70)	3.63 (3.78–3.63)	3.80 (3.94–3.80)	3.80 (3.94–3.80)	3.50 (3.63–3.50)
Completeness (%)	100 (100)	100 (99.9)	99.0 (100)	98.0 (99.3)	100 (100)
Total reflections	204,935	260,474	280,672	212,408	596,530
Unique reflections	34,832	36,610	36,493	35,008	49,289
R_{sym} (%)	8.6 (44.4)	10.1 (45.0)	10.1 (44.2)	8.4 (53.8)	8.7 (54.6)
R_{work} (%)	27.2	24.5	28.3	28.4	25.7
R_{free} (%)	33.0	32.2	34.4	33.8	32.3

[1]Department of Molecular and Cell Biology, University of California, Berkeley, CA 94720–3202, USA. [2]Berkeley Center for Structural Biology, Physical Biosciences Division, Lawrence Berkeley National Laboratory, Berkeley, CA 94720, USA.

*Present address: Department of Chemistry and Biochemistry, University of Oklahoma, Norman, OK 73019, USA.

†To whom correspondence should be addressed. E-mail: dek@uclink4.berkeley.edu

is surrounded with many hydrophobic residues, including 12 well-conserved phenylalanine residues, each protomer contributing Phe^{386}, Phe^{388}, Phe^{458}, and Phe^{459}. These residues are involved in drug binding, as seen below, suggesting that the binding is mainly governed by hydrophobic and perhaps also aromatic $\pi-\pi$ interactions. Below we describe the structure of ligand-AcrB complexes. Another notable feature is that all these ligands bind more or less to the area that should be near the outer surface of the lipid bilayer, if, as seems likely, this cavity is filled with the bilayer.

In the R6G complex structure, the loop regions between helices α3 and α4, and helices α5 and α6 form a ligand-binding domain in the large cavity facing the cytoplasm (Figs. 1 and 2). The ligand-binding cavity is extensive and occupies most of the upper half of the transmembrane region in the central cavity. Its total volume is ~5000 Å^3. The binding site in one subunit contains, within 6 Å distance from the ligand, Phe^{386}, Ala^{385}, Leu^{25}, Val^{382}, Lys^{29}, and Phe$^{386'}$ from the neighboring subunit (the residue number with the prime symbol indicates a residue from another subunit). AcrB is a homotrimer, and each R6G molecule binds to the area corresponding to the border between the two neighboring subunits. These three identical sites face each other in the central cavity. They appear to assist and interact with each other, forming a large, single binding pocket to bind three drug molecules. Lys^{29} located at the vestibule in each subunit appears to point its side chain toward the ester group of each substrate. It is noteworthy that all other residues within 6 Å of the bound ligand are hydrophobic amino acids, suggesting the importance of the hydrophobic and possibly van der Waals interactions in drug binding. The three bound ligand molecules appear to interact with each other to stabilize the final configuration.

In the AcrB-Et complex, Et binds at a site that is distinct from but partially overlaps with the R6G binding site. Compared with the R6G binding, Et is bound ~6 Å above the R6G binding site (compare Fig. 1, A and B), and its binding site is closer to the vestibule than that of R6G. The amino acid residues within 6 Å of Et include Phe^{386} and Ala^{385} from one subunit and Phe$^{386'}$ from the neighboring subunit; Phe^{388} is located slightly farther away (7 to 8 Å) (Fig. 2B). Et is close to Phe^{386} (~4 Å). The phenyl moiety of Et is bound above Phe$^{386'}$, interacting closely with this residue. In this way, the bound Et molecule is sandwiched between two subunits of the transporter. As with R6G, most of these interactions are hydrophobic. In the binding pocket, the carbonyl oxygen of Phe^{386} is close to one of the amino groups of Et (3.6 Å), and may contribute to the neutralization

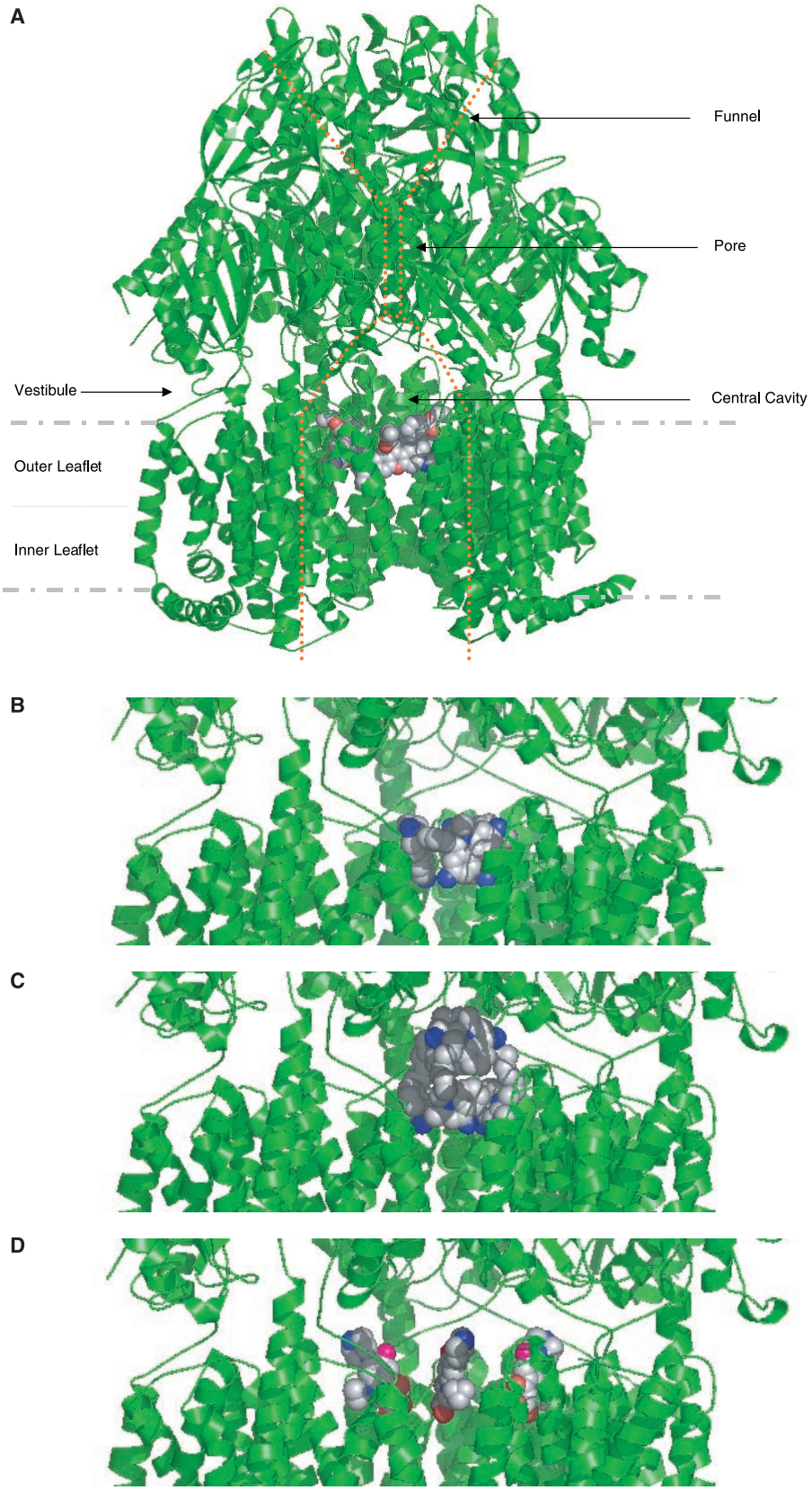

Fig. 1. Structures of the trimeric AcrB transporter with bound ligands viewed from the side parallel to the membrane. (**A**) AcrB with three bound R6G molecules. The figure shows the transmembrane domain (inner and outer leaflets), the periplasmic domain, and the location of cavity, vestibule, pore, and funnel (*8*). The drugs are bound approximately at the level of the outer surface of the membrane lipid bilayer. (**B**) through (**D**) show the center of the side view in (A), with bound Et, Dq, and Cip molecules. This figure and Fig. 2 were prepared with PyMOL (*22*).

of the formal charge of the substrate. The three bound Et molecules are ~3.2 Å apart from one another, indicating that these ligands interact strongly in the central cavity.

The three bound Dq molecules occupy a large portion of the upper part of the binding pocket (Fig. 1C). Within 6 Å of a Dq molecule, we find two acidic residues, Asp^{99} and Asp^{101}, as well as Ile^{102}, close to the quinolinium moiety at the top (i.e., closer to the outer membrane) (Fig. 2C). Interaction with the two acidic residues appears to neutralize the formal positive charge of the quinolinium at the top. Asp^{99} is highly conserved (*10*), and this observation shows the importance of this residue in recognizing cationic drugs. This quinolinium group at the top forms a tight cluster with two other quinolinium moieties from the other two drug molecules. In contrast, the bottom part of the ligand, containing the second quinolinium moiety, is not within 6 Å of any residues on the cavity wall, although it is ~6.3 Å away from the two phenylalanine residues (Phe^{386} and $Phe^{386'}$) from the two neighboring subunits. Thus the Dq contacts again are dominated by hydrophobic interactions, but the top quinolinium moiety has a strong electrostatic interaction. Also the drug-to-drug interaction appears to be quite tight in this complex.

As with R6G, the Cip molecule is bound between two protein subunits. Residues within 6 Å of the bound ciprofloxacin include Phe^{458}, Phe^{459}, and $Lys^{29'}$, $Leu^{25'}$ and $Ala^{385'}$ from the neighboring subunit (Figs. 1D and 2D). In the complex, again most of the interaction with the ligand is hydrophobic. The cyclopropyl group of the drug molecule interacts with Phe^{458} and Phe^{459} (the distance to the latter is 3.3 Å). From the neighboring subunit, the side chains of $Leu^{25'}$ and $Lys^{29'}$ are close to the ring nitrogen of the quinolone moiety. The fairly close distance (5 Å) between the ε-amino group of $Lys^{29'}$ and the electron-poor ring nitrogen [an

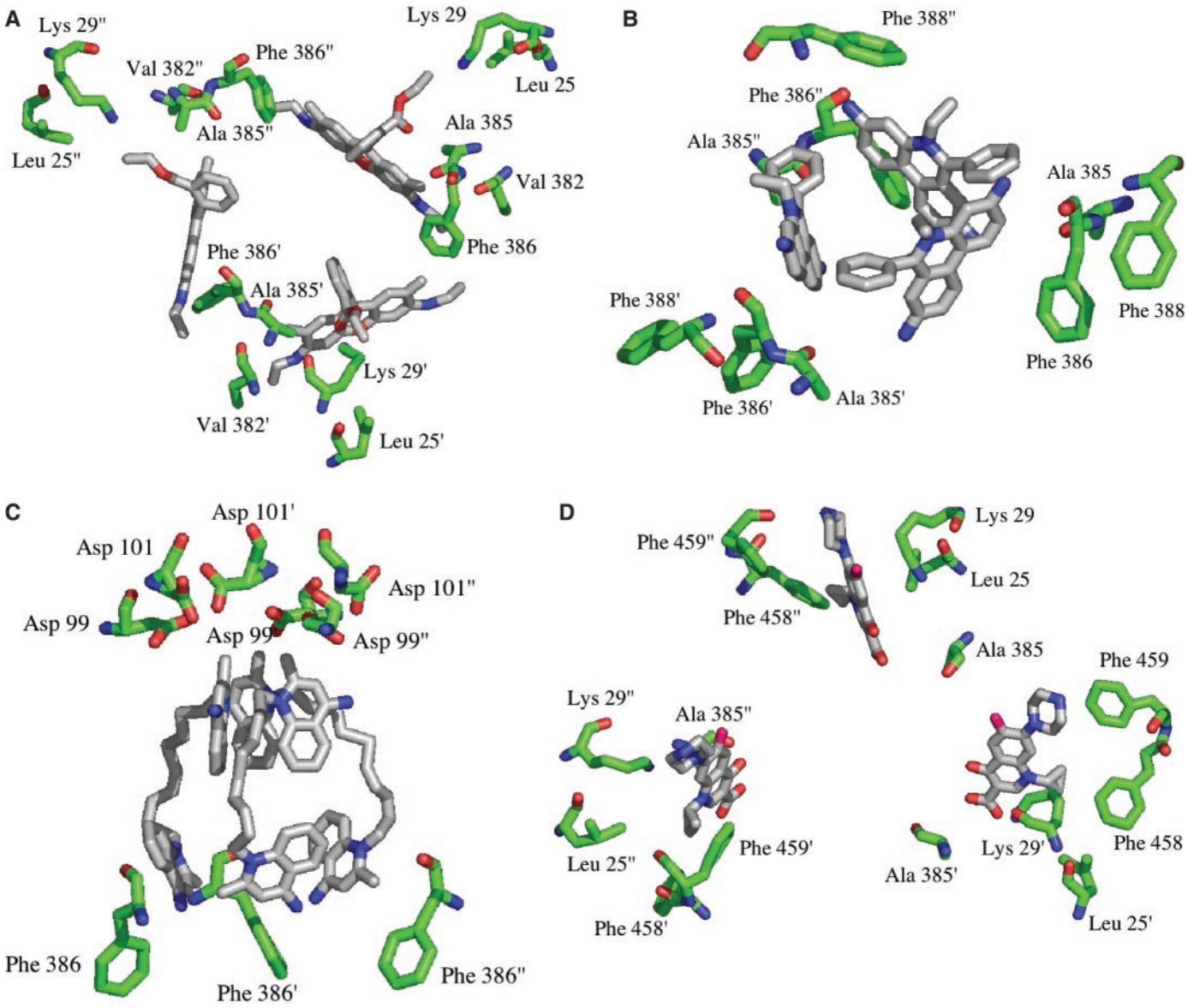

Fig. 2. The binding sites for the four ligands. Amino acid residues within 6 Å of the bound ligand molecules are shown. With the exception of (C), the view is approximately from the top (periplasmic side) of the trimer. Unmarked, primed, and double-primed residues, respectively, belong to the three subunits of the AcrB trimer. (**A**) R6G-binding site. (**B**) Et-binding site, including Phe^{388} that is slightly farther away (see text). (**C**) Dq-binding site. The side view shows the binding of the two quinolinium moieties within each Dq molecule (as in Fig. 1). The phenylalanine residues interacting with the bottom quinolinium moieties are shown even though they are 6.3 Å away from the ligand. Ile^{102} is not shown to avoid cluttering the figure. (**D**) Cip-binding site.

analog, 1-methyl-4-quinolone, has a pK_a of 2.46 (*11*)] also suggests some dipolar contributions. The carbonyl oxygen of Ala$^{385'}$ is also 5 Å away from one of the carboxyl oxygens of Cip, and these two groups may interact with the intervening water molecule. The geometry of the other carboxyl oxygen and the 4-carbonyl oxygen of Cip suggests that the carboxyl oxygen is protonated and that these atoms are parts of the six-membered, hydrogen-bonded ring that also includes C3 and C4 of the quinoline ring (*12*).

The details of these binding interactions confirm and extend the observation on the binding of various ligands to the regulatory proteins BmrR and QacR (*4*, *5*). Thus the binding cavity is large, and each ligand binds to a different part of the cavity by using a different set of amino acid residues. There are, however, features that we did not expect from the studies of the binding proteins: (i) The binding cavity is extremely large and binds several molecules of ligands at the same time. With the multidrug transporter MdfA of *E. coli*, kinetic studies suggested the simultaneous binding of chloramphenicol and tetraphenylphosphonium (*13*). The present result indeed supports such a mechanism of binding. (ii) With the regulatory protein QacR, ligand binding involved the enlargement of the binding site by the expulsion of two tyrosine side chains (*5*). No drastic enlargement was seen in the already very large cavity of trimeric AcrB. (iii) With QacR, electrostatic interactions played a very important role in the binding of cationic dyes (*5*). With AcrB, the binding of the dyes R6G and Et appeared to involve mostly hydrophobic interactions rather than strong electrostatic interactions. This result is probably due to the large size of the binding pocket, possible interaction between the drug molecules, and the delocalized nature of the charge in these dyes. In contrast, for the cationic disinfectant Dq, with its more localized charges, the electrostatic interaction with acidic amino acid residues was apparent, at least with the quinolinium moiety on top, as described above. Unexpectedly, there was no obvious electrostatic stabilization of the quinolinium moiety at the bottom. In view of its location close to the surface of the presumed bilayer within the cavity (Fig. 1), however, this moiety (as well as other cationic moieties such as the protonated piperazine 4-N in Cip) may be stabilized by its interaction with the head groups of acidic phospholipids.

Comparison of the R6G-bound structure with the drug-free structure reveals that binding of the drug triggers a 1° rigid-body rotation in each subunit. The axis of rotation, passing through the side of each subunit, is approximately parallel to the plane of the lipid-bilayer. This motion enlarges the diameter of the periplasmic domain by ~2.5 Å. The rotation is probably triggered by interactions between the ligand and the transporter and was seen also in the structure of Et-, Dq-, and Cip-bound AcrB (see reference 1 in supporting online material).

Previous biochemical studies have shown that AcrB exists as a complex with the periplasmic protein AcrA (*14*). These two proteins, presumably, interact specifically in the periplasm. The role of AcrA, which is absolutely required for transport, is still not clear. It is possible that the 1° rigid-body rotation of AcrB brings the periplasmic domain of AcrB closer to AcrA and that this triggers the conformational changes of these proteins that further trigger the drug transport. Hydrodynamic and electron crystallography studies of AcrA (*15*, *16*) indicate that AcrA is an elongated, asymmetric protein. Such a flexible protein is ideal for amplifying transmembrane signal, because a small change at one end of the protein may eventually cause a large conformational change at the other end.

With the binding of R6G and Dq, we see a downward movement of a loop between residues 300 and 310 in the periplasmic domain, which causes the Arg^{307} side chain to flip downward and shift toward the center of the vestibule.

The drug molecules that are bound to the central cavity are probably pushed out through the periplasmic domains of AcrB, into the α-helical tunnel of TolC, and finally into the medium (*3*). The most direct route for drug extrusion may be through the central pore, which is formed by the pore helix in the periplasmic domain, residues 102 to 115 (*6*). In the unliganded as well as liganded AcrB, these residues make direct coil-coil interaction right at the center among the three subunits, and the pore is thus closed. Possibly the proton flux that follows the ligand binding produces a large conformational change of AcrB that leads to the opening of the pore and to the elevator-type mechanism of drug extrusion.

Recent genetic studies identified domains and residues that appear to be important in the substrate efflux in AcrB and its homologs. Thus, domain swapping (*17*, *18*) and point mutation (*19*) studies both showed that the periplasmic domain plays a major role in determining the substrate specificity of these pumps. Yet most of the residues identified as parts of drug-binding sites in this study come from the transmembrane domain, with the exception of Asp^{99}, Asp^{101}, and Ile^{102}. This is partly because drugs presumably traverse the vestibule, which primarily belongs to the periplasmic domain, to reach the cavity, and much discrimination may be exerted in the entry into and traversal through this channel. Also, the binding seen here represents only the first step of the efflux process, and drugs may interact with other sites before their final extrusion into the tunnel of the TolC protein.

The liganded structures show that the diverse chemicals were able to bind complementary polar and hydrophobic groups in the large central cavity in the efflux transporter firmly (but transiently, because the chemicals must be transported out). The observation that the ligands induce the same 1° rotation of

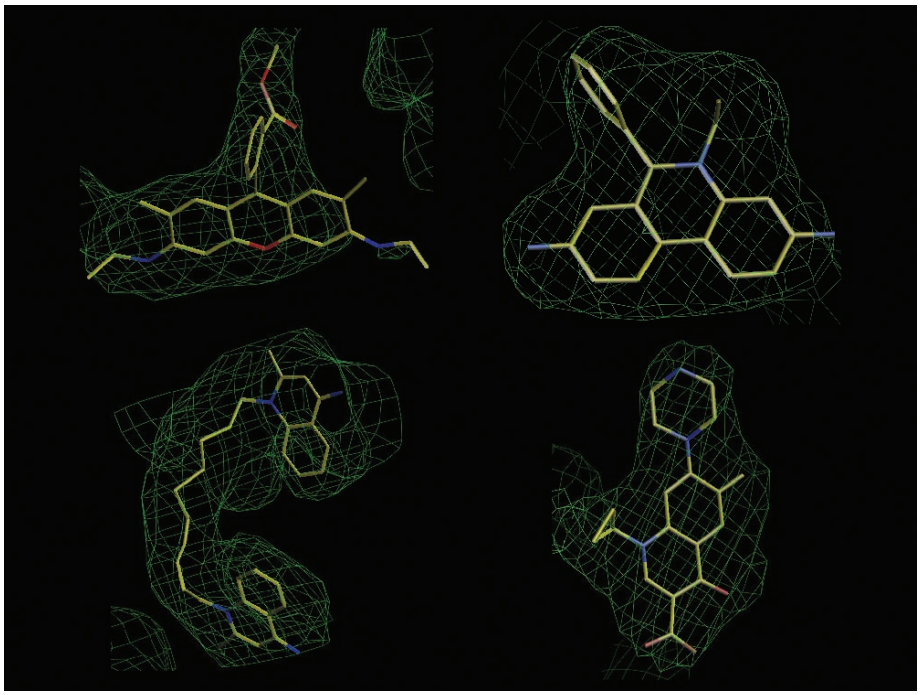

Fig. 3. The final $2F_{obs} - F_{calc}$ electron density maps (green) of the bound ligands contoured at 1.5σ. (**Top left**) Rhodamine 6G. (**Top right**) Ethidium. (**Bottom left**) Dequalinium. (**Bottom right**) Ciprofloxacin.

the protein indicates that all participate in a thermodynamic shift toward the same conformational state. In this regard, that four different ligands induce a similar conformational change in the transporter, a finding that is consistent with the hypothesis (*20*) that the induced conformational state reflects evolutionary changes that select for amino acid residue interactions that optimize the kinetic and thermodynamic values needed for the conformational change.

It has been proposed earlier by one of us (*2*) that amphiphilic drug molecules partition partly into the outer leaflet of the cytoplasmic membrane, diffuse laterally within the leaflet, and eventually are captured by AcrB. The location of the binding site fits perfectly with this hypothesis. The hydrophilic head group of the drug would travel through the vestibules (*8*) (Fig. 1). Below the vestibule, there is a wide opening between the neighboring subunits in the upper part of the transmembrane domain. The hydrophobic part of the drugs may diffuse through this opening, presumably filled with the continuation of the outer leaflet of the lipid bilayer, to reach the binding sites seen in this study, close to the outer surface of the putative lipid bilayer within the cavity. The presence of the large substrate-binding cavity in AcrB is also reminiscent of the similarly large cavity in the low-resolution structure of mammalian P-glycoprotein (*21*).

References and Notes

1. M. M. Gottesman, *Annu. Rev. Med.* **53**, 615 (2002).
2. H. Nikaido, *J. Bacteriol.* **178**, 5853 (1996)
3. H. I. Zgurskaya, H. Nikaido, *Mol. Microbiol.* **37**, 219 (2000).
4. E. E. Zheleznova, P. N. Markham, A. A. Neyfakh, R. G. Brennan, *Cell* **96**, 353 (1999).
5. M. A. Schumacher *et al.*, *Science* **294**, 2158 (2001).
6. D. Ma *et al.*, *J. Bacteriol.* **175**, 6299 (1993).
7. H. I. Zgurskaya, H. Nikaido, *Proc. Natl. Acad. Sci. U.S.A.* **96**, 7190 (1999).
8. S. Murakami, R. Nakashima, E. Yamashita, A. Yamaguchi, *Nature* **419**, 587 (2002).
9. Materials and Methods are available as supporting material on *Science* Online.
10. I. T. Paulsen, M. H. Brown, R. A. Skurray, *Microbiol. Rev.* **60**, 575 (1996).
11. A. Albert, J. N. Phillips, *J. Chem. Soc.* 1294 (1956).
12. H. Nikaido, D. G. Thanassi, *Antimicrob. Agents Chemother.* **37**, 1393 (1993).
13. O. Lewinson, E. Bibi, *Biochemistry* **40**, 12612 (2001).
14. H. I. Zgurskaya, H. Nikaido, *J. Bacteriol.* **182**, 4264 (2000).
15. H. I. Zgurskaya, H. Nikaido, *J. Mol. Biol.* **285**, 409 (1998).
16. A. J. Avila-Sakar *et al.*, *J. Struct. Biol.* **136**, 81 (2001).
17. C. Elkins, H. Nikaido, *J. Bacteriol.* **184**, 6490 (2002).
18. E. Tikhonova, Q. Wang, H. Zgurskaya, *J. Bacteriol.* **184**, 6499 (2002).
19. W. Mao *et al.*, *Mol. Microbiol.* **46**, 889 (2002).
20. E. W. Yu, D. E. Koshland Jr., *Proc. Natl. Acad. Sci. U.S.A.* **98**, 9517 (2001).
21. M. F. Rosenberg, R. Callaghan, R. C. Ford, C. F. Higgins, *J. Biol. Chem.* **272**, 10685 (1997).
22. W. L. DeLano, The PyMOL Molecular Graphics System (DeLano Scientific, San Carlos, CA, 2002); www.pymol.org.

23. We thank G. Meigs and H. Petras for technical support at the Advanced Light Source. Initial crystal screens were performed at the Stanford Synchrotron Radiation Laboratory. We also thank T. Alber and Y. Koshland for proofreading the manuscript. Supported by NIH grants AI 09644 (to H.N.) and an NIH postdoctoral fellowship (to E.W.Y.). Coordinates have been deposited with the Protein Data Bank. Accession codes for the unliganded, AcrB-R6G, AcrB-Et, AcrB-Dq, and AcrB-Cip structures are 1OY6, 1OY8, 1OY9, 1OYD, and 1OYE, respectively.

Supporting Online Material

www.sciencemag.org/cgi/content/full/300/5621/976/DC1
Materials and Methods
Fig. S1
References

5 February 2003; accepted 8 April 2003

Molecular Architecture of the Multiprotein Splicing Factor SF3b

Monika M. Golas, Bjoern Sander, Cindy L. Will, Reinhard Lührmann, Holger Stark*

The splicing factor SF3b is a multiprotein complex essential for the accurate excision of introns from pre-messenger RNA. As an integral component of the U2 small nuclear ribonucleoprotein (snRNP) and the U11/U12 di-snRNP, SF3b is involved in the recognition of the pre-messenger RNA's branch site within the major and minor spliceosomes. We have determined the three-dimensional structure of the human SF3b complex by single-particle electron cryomicroscopy at a resolution of less than 10 angstroms, allowing identification of protein domains with known structural folds. The best fit of a modeled RNA-recognition motif indicates that the protein p14 is located in the central cavity of the complex. The 22 tandem helical repeats of the protein SF3b155 are located in the outer shell of the complex enclosing p14.

The precise excision of introns from pre-messenger (pre-mRNA) is catalyzed by the spliceosome (*1*). This large protein-RNA complex is assembled on pre-mRNA by the stepwise association of several snRNPs. Two different spliceosomes exist in mammals: the major (U2-type) and the minor (U12-type) spliceosomes (*2*). They recognize different classes of splice sites and differ in snRNP composition. U1, U2, and U4/U6·U5 snRNPs are components of the major spliceosome, whereas the minor spliceosome contains the U11/U12 di-snRNP and the U4atac/U6atac·U5 tri-snRNP. Little is known about the molecular architecture and three-dimensional (3D) structure of snRNPs and spliceosomal complexes. The first 3D structure of a complete snRNP particle (U1) was determined only recently with the use of single-particle electron cryomicroscopy (cryo-EM) (*3*).

The protein complex SF3b takes part in both splicing pathways as an integral part of the U2 snRNP and the U11/U12 di-snRNP (*4*). SF3b has a mass of ~450 kdalton, consists of seven proteins (table S1) (*5*–*8*), and is absolutely required for pre-mRNA splicing. SF3b plays an essential role during the assembly of the so-called prespliceosome and contributes to the recognition of the intron's branch point. During spliceosome assembly, several SF3b proteins can be cross-linked to the pre-mRNA in the vicinity of the branch point (*9*, *10*). The SF3b protein p14 cross-links directly to the branch-point adenosine of the intron after the integration of the U2 snRNP into the prespliceosome, and it can be cross-linked to the same point in subsequently formed complexes, including the catalytically active spliceosomal C complex (*11*, *12*). Because the branch-point adenosine acts as the nucleophile for the first catalytic step of splicing, p14 is thought to be located close to the catalytic center of the spliceosome.

High-resolution x-ray or nuclear magnetic resonance structures are not yet available for any of the SF3b proteins. However, several known structural motifs of SF3b proteins have been found by sequence alignment (table S1). The largest of these proteins is SF3b155, and its C terminus was found to contain 22 HEAT repeats (*13*). The x-ray structures of the A subunit of protein phosphatase 2A, importin-β, and eukaryotic initiation factor 4G have revealed that HEAT repeats form tandem helical repeats (*14*–*16*). A single HEAT repeat consists of ~40 amino acids forming two antiparallel α helices in most cases and 3_{10} helices in a few rare cases. The repetition of many such units results in a curved ladder-like structure (*14*–*16*). Two other SF3b proteins have been identified as containing RNA-recognition motif (RRM) domains. One of these two proteins is p14, which consists mainly of one RRM (*7*). Another SF3b protein, SF3b49, has been found to contain two closely adjacent RRMs in its sequence (*17*). RRMs contain ~90 amino acid residues, and the globular RRM domain consists of four β strands and two α helices in the order β1-α1-β2-β3-α2-β4 (*18*). SF3b is a structural component of the U2 snRNP, the

Max Planck Institute for Biophysical Chemistry, Am Fassberg 11, 37077 Göttingen, Germany.

*To whom correspondence should be addressed. E-mail: holger.stark@mpibpc.mpg.de